Hyposulfatemia, growth retardation, reduced fertility, and seizures in mice lacking a functional NaS_i-1 gene

Paul A. Dawson*, Laurent Beck†, and Daniel Markovich*‡

*School of Biomedical Sciences, University of Queensland, Brisbane 4072, Australia; and †Institut National de la Santé et de la Recherche Médicale U426, Faculté de Médecine Xavier Bichat, 75018 Paris, France

Edited by Joseph F. Hoffman, Yale University School of Medicine, New Haven, CT, and approved September 3, 2003 (received for review March 5, 2003)

Inorganic sulfate is required for numerous functions in mammalian physiology, and its circulating levels are proposed to be maintained by the Na^+–SO_4^{2-} cotransporter, (NaS_i-1). To determine the role of NaS_i-1 in sulfate homeostasis and the physiological consequences in its absence, we have generated a mouse lacking a functional NaS_i-1 gene, *Nas1*. Serum sulfate concentration was reduced by >75% in *Nas1*$^{-/-}$ mice when compared with *Nas1*$^{+/+}$ mice. *Nas1*$^{-/-}$ mice exhibit increased urinary sulfate excretion, reduced renal and intestinal Na^+–SO_4^{2-} cotransport, and a general growth retardation. *Nas1*$^{-/-}$ mouse body weight was reduced by >20% when compared with *Nas1*$^{+/+}$ and *Nas1*$^{+/-}$ littermates at 2 weeks of age and remained so throughout adulthood. *Nas1*$^{-/-}$ females had a lowered fertility, with a 60% reduction in litter size. Spontaneous clonic seizures were observed in *Nas1*$^{-/-}$ mice from 8 months of age. These data demonstrate NaS_i-1 is essential for maintaining sulfate homeostasis, and its expression is necessary for a wide range of physiological functions.

Inorganic sulfate (SO_4^{2-}) is an abundant anion in mammalian plasma and is essential for numerous physiological functions (1). SO_4^{2-} conjugation is an important step in the biotransformation of xenobiotics such as steroids, antiinflammatory agents, adrenergic stimulants and blockers, analgesics, and, in most cases, leads to an increase in their urinary excretion (2). SO_4^{2-} is also required for the activation of many endogenous compounds such as heparin, heparan sulfate, dermatan sulfate, and bile acids (3). In addition, sulfation of structural components such as glycosaminoglycans and cerebroside sulfate is essential for the maintenance of normal structure and function of tissues (4). Disturbances of SO_4^{2-} metabolism and transport have been associated with human syndromes and diseases, including metachromatic leukodystrophy, Hunter's syndrome, Morquio's syndrome, Maroteaux–Lamy syndrome, multiple-sulfohydrolase deficiency, and osteochondrodysplasias (5, 6). However, despite its importance in the body, SO_4^{2-} levels are rarely measured in a clinical setting and there remains areas in which knowledge of its significance is still lacking, or is at most, minimal.

In humans, SO_4^{2-} absorption is initiated in the small intestine and its homeostasis is proposed to be maintained through renal tubular mechanisms (7). SO_4^{2-} is freely filtered in the glomerulus and is actively reabsorbed in the proximal tubule. Renal proximal tubular SO_4^{2-} reabsorption is mediated by entry through the brush-border membrane (BBM) by a Na^+–SO_4^{2-} cotransporter (NaS_i-1), and exit through the basolateral membrane by an anion exchanger, Sat-1 (1). The NaS_i-1 transporter is expressed primarily in the kidney and intestine (8) and has been proposed to play a major role in maintaining serum SO_4^{2-} concentrations within the normal physiological range of 0.33–0.47 mmol/liter in humans (9–11). In recent years, a growing body of experimental evidence has demonstrated that various dietary and hormonal conditions alter serum SO_4^{2-} levels by means of the regulation of NaS_i-1 (1, 12). The positive and negative regulatory effects of these factors on NaS_i-1 mRNA and protein levels and Na^+–SO_4^{2-} cotransport demonstrate that NaS_i-1 is highly regulated by its external environment and most likely plays an important role in maintaining SO_4^{2-} homeostasis.

Recently, we cloned both the mouse and human NaS_i-1 genes, designated *Nas1* and *NAS1*, respectively (13, 14). These genes are structurally similar, with each containing 15 exons and 14 introns spread over ≈80 kb. The *Nas1* gene was mapped to mouse chromosome 6, in a region of conserved synteny with the human *NAS1* gene on chromosome 7q31-q32. Interestingly, other SO_4^{2-} transporter genes including DRA (down-regulated in colonic adenomas and adenocarcinomas) (15) and SUT-1 (a Na^+–SO_4^{2-} cotransporter from human high endothelial venules) (16), are present in close proximity to *NAS1*, suggesting this genomic region may be important for coordinating the regulation of SO_4^{2-} homeostasis.

To define the role of NaS_i-1 in the maintenance of SO_4^{2-} homeostasis, we have generated mice in which the NaS_i-1 gene was disrupted by targeted mutagenesis.

Methods

Targeting Vector Construction. Fragments of *Nas1* were isolated from a genomic clone (λ5) (13) and used to create the targeting vector shown in Fig. 1*A*. A 3.7-kb *Xho*I–*Hin*dIII fragment containing exon 3 and a 2.3-kb *Pst*I fragment of intron 6 were subcloned on either side of the phosphoglycerate kinase–neomycin resistance (Neo^r) expression cassette of the pPNT vector (17). On homologous recombination, this vector deleted ≈3 kb of *Nas1* genomic sequences, including exons 4–6. Deletion of exons 4–6 introduced a subsequent frameshift and premature stop codon (Fig. 2*A*).

Generation and Identification of *Nas1*$^{-/-}$ Mice. The targeting construct was electroporated into C1368 mouse embryonic stem (ES) cells (a gift from Dr. G. Kay, Queensland Institute of Medical Research, Brisbane, Queensland, Australia). Transfectants were selected in medium containing 300 μg/ml G418 and 0.2 μM 1-(2′-deoxy-2′-fluoro-β-D-arabinofuranosyl)-5-iodouracil for 5 days and then for 3 more days with G418 alone. Clones that had undergone homologous recombination were identified by Southern blot analysis by using an external 1.1-kb *Xba*I–*Xho*I fragment of intron 2 as a probe (Fig. 1*A*). The intron 2 probe detected a 4.8-kb *Xba*I wild-type allele fragment and a 6.6-kb *Xba*I recombinant allele fragment. Positive clones were further analyzed by using PCR to amplify a 13.5-kb recombinant allele fragment. PCR was performed by using primer P1 (5′-GAATGGGCTGACCGCTTCCT-3′) in the Neo^r gene cassette and antisense primer P5 (5′-CATCTTTCTTGACACTTTCCCTTT-3′) in exon 7 (Fig. 1*A*). Positive ES cell clones (3 of 300 clones) were injected into C57BL/6J blastocysts that were implanted into foster mothers (Transgenic Animal Service of Queensland, Queensland, Australia, and Queensland Institute of Medical Research, Brisbane, Queensland, Australia). Chimeric mice were generated from two different clones, and the F2 generation mice were used in the

This paper was submitted directly (Track II) to the PNAS office.

Abbreviations: NaS_i-1, Na^+-sulfate cotransporter; BBM, brush-border membrane; BBMV, BBM vesicle; ES, embryonic stem; Neo^r, neomycin resistance; IGFI, insulin-like growth factor I; ST, sulfotransferase.

‡To whom correspondence should be addressed at: Department of Physiology and Pharmacology, School of Biomedical Sciences, University of Queensland, St. Lucia, Queensland 4072, Australia. E-mail: d.markovich@uq.edu.au.

www.pnas.org/cgi/doi/10.1073/pnas.2231298100

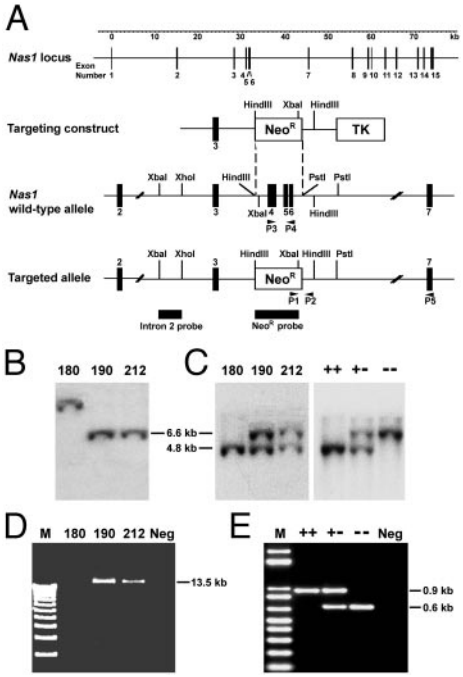

Fig. 1. Targeted disruption of *Nas1*. (*A*) *Nas1* targeting strategy. Exons (black boxes), restriction sites, probes, and primers (P1–P5) are shown. Neo^R, neomycin resistance. TK, thymidine kinase sequences. (*B*) Southern analysis of *Xba*I-digested DNA from ES cell clones. The Neo^R probe detected a 6.6-kb fragment from clones 190 and 212, but, presumably, a random insertion in clone 180. (*C*) Southern analysis of *Xba*I-digested DNA from ES cell clones and from *Nas1*$^{+/+}$, *Nas1*$^{+/-}$, and *Nas1*$^{-/-}$ mice. The intron 2 probe detected 4.8-kb wild-type and 6.6-kb targeted allele fragments. (*D*) Forward (P1) and reverse (P5) primers amplified a 13.5-kb product in ES cell clones 190 and 212. (*E*) PCR genotyping of *Nas1*$^{+/+}$, *Nas1*$^{+/-}$, and *Nas1*$^{-/-}$ mice. Primers P3 and P4 amplified a 0.9-kb wild-type fragment; P1 and P2 amplified a 0.6-kb targeted allele product.

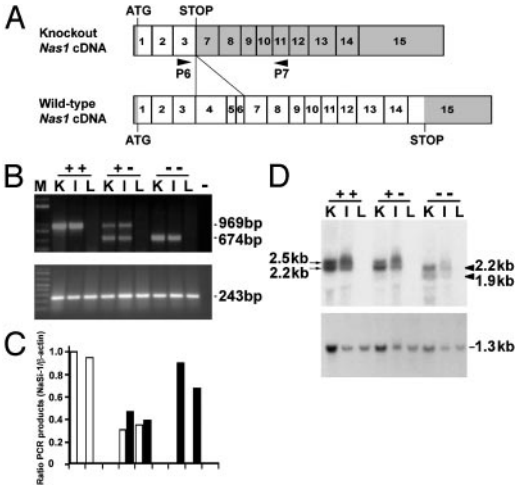

Fig. 2. Analysis of NaS$_i$-1 mRNA. (*A*) A schematic of NaS$_i$-1 cDNA and the predicted knockout cDNA lacking exons 4–6. Exons 1–15 (boxes) and protein coding sequences (white portions) of wild-type (1,779 nucleotides) and NaS$_i$-1 knockout (363 nucleotides) cDNA. (*B*) Total RNA from kidney (K), ileum (I), and liver (L) was RT-PCR-amplified. A 969-bp wild-type product and a 674-bp knockout NaS$_i$-1 cDNA product (*Upper*) were amplified by using primers P6 and P7. A 243-bp product (*Lower*) was amplified by using β-actin primers. M, molecular mass ladder. −, negative control. (*C*) Densitometric analysis of the NaS$_i$-1 PCR products in *B*, representative of two other experiments with similar data. White bars, wild-type product; filled bars, knockout product. (*D*) Northern analysis of RNA from kidney, ileum, and liver of *Nas1*$^{+/+}$, *Nas1*$^{+/-}$, and *Nas1*$^{-/-}$ mice. RNA was hybridized sequentially with a ^{32}P-labeled NaS$_i$-1 cDNA (*Upper*) showing the two *Nas1*$^{+/+}$ transcripts (arrows, 2.5 and 2.2 kb) and the two *Nas1*$^{-/-}$ truncated transcripts (arrowheads, 2.2 and 1.9 kb), and GAPDH cDNA (*Lower*).

present study. Tail biopsies were genotyped by PCR and Southern blot analysis (see below). To produce *Nas1*$^{-/-}$ mice, heterozygous offspring were intercrossed. Studies were performed on mice with a mixed genetic background (129Sv and C57BL/6J). Mice were maintained on a 12-h light-dark cycle and fed ad libitum on standard rodent chow (diet no. AIN93G; Glen Forrest Stockfeeders, Glen Forrest, Western Australia) in accordance with the guidelines of the University of Queensland Animal Ethics Committee.

Genotyping of Mice. Mice were genotyped by PCR and Southern blot analysis. PCR was performed by using primer P1 and antisense primer P2 (5′-CTGGATTAGACAGAAGCAAC-3′) in intron 6 to amplify a 0.6 kb fragment of the recombinant *Nas1* allele (Fig. 1*A*). Primer P3 (5′-CACTGCCTTCTTATCTATGTGG-3′) in exon 4 and antisense primer P4 (5′-CATCTTTCTTGACACTTTC-CCTTT-3′) in exon 6 were used to amplify a 0.9-kb fragment of the wild-type *Nas1* allele (Fig. 1*A*). Cycle parameters were: 95°C for 10 seconds; followed by 35 cycles of 95°C for 10 seconds, 60°C (P1/P2) or 55°C (P3/P4) for 30 seconds, and 68°C for 5 min. Genomic DNA was digested with *Xba*I and analyzed by Southern blot hybridization using intron 2 probe (Fig. 1*A*). Expected sizes of fragments for the wild-type and disrupted alleles are 4.8 and 6.6 kb, respectively.

Analysis of RNA. Total RNA (10 μg) was separated on a 1% agarose formaldehyde gel in Mops buffer and transferred to Hybond-XL nylon membranes (Amersham Pharmacia). The blots were probed with a 1.2-kb NaS$_i$-1 cDNA and a 0.6-kb mouse GAPDH cDNA probe. For RT-PCR, total RNA (2 μg) was reverse transcribed by using random hexamers and Moloney murine leukemia virus reverse transcriptase (Progen, Brisbane, Queensland, Australia) as recommended by the manufacturer. Primer P6 (5′-CTTTCACCT-TCTGCTAATTGGA-3′) in exon 3 and antisense primer P7 (5′-GTCATTTTTGTCAGTTTCTTGGC-3′) in exon 11 (Fig. 2*A*) were used to amplify NaS$_i$-1 cDNA fragments. Primers 5′-CGTGGGCCGCCCTAGGCACCA-3′ and 5′-TTGGCCT-TAGGGTTCAGGGGGG-3′ were used for detection of β-actin cDNAs (18).

BBM Vesicle (BBMV) Preparation and Transport Studies. BBMVs were isolated from mouse kidneys and ilea by using described methods (19). The uptakes of SO_4^{2-} (0.1 mM) and glucose (0.1 mM), each performed in quadruplicate, were measured at 10 s and 90 min in media containing either 100 mM NaCl or 100 mM KCl by the rapid filtration technique (19).

Blood and Urinary Analysis. Serum and urine SO_4^{2-}, PO_4^{2-}, Ca^{2+}, and creatinine concentrations were assayed on an Hitachi 917 automatic analyzer (Hitachi, Tokyo). The fractional excretion index (FEI) of SO_4^{2-}, PO_4^{2-}, and Ca^{2+} was calculated as follows: (serum creatinine $\times$ urine SO_4^{2-}, PO_4^{2-}, or Ca^{2+})/(urine creatinine $\times$ serum SO_4^{2-}, PO_4^{2-}, or Ca^{2+}). The serum concentration of insulin-like growth factor I (IGFI) was measured by using a radioimmunoassay kit (Bioclone, Marrickville, New South Wales, Australia). Serum Na^+, K^+, and Cl^- concentrations were assayed by a commercial pathology laboratory (Sullivan Nicolaides Pathology, Taringa, Queensland, Australia) using a Vitros 250 chemistry analyzer (Ortho-Clinical Diagnostics, New York). Whole blood and urine pH was measured with an ISFET pH meter (Shindengen, Camarillo, CA). Urine total protein levels were quantitated by using a Microprotein-PR kit (Sigma). Serum bile acids were HPLC-separated by using a Waters X-Terra MS C18 3.5-μm 2.1 $\times$ 150-mm column at a flow rate of 0.2 ml/min. Unpaired Student's *t* tests were used to analyze all blood and urinary data. Systolic blood pressure

was measured three to four times per mouse by using an MLT125/M computerized tail-cuff apparatus (ADInstruments, Castle Hill, New South Wales, Australia).

Histopathological Analysis. Tissues were dissected into ≈50 volumes of 10% buffered formalin and fixed for 3 days before paraffin embedding. Tibia samples were decalcified in Gooding and Stewart's solution (2% formalin and 10% formic acid) at 4°C for 4–7 days before embedding in paraffin. Embedded tissue was sectioned, hematoxylin/eosin stained, and examined by light microscopy. Bone length was measured from digital images of excised femurs by using NIH IMAGE software.

Sulfotransferase (ST) Assays. Liver cytosol preparations and phenol ST assays were performed as described (20). Livers were homogenized on ice in 5 volumes of 10 mM phosphate buffer (pH 7.4) containing 1 mM DTT and 10% glycerol. Liver homogenates were centrifuged at 100,000 × *g* for 1 h at 4°C. The supernatant fraction (cytosol) was removed and assayed for protein concentration (21). The cytosolic fractions were diluted 10-fold in 10 mg/ml BSA. Phenol ST activity was assayed in 10 mM potassium phosphate (pH 7.4) at 37°C for 30 min with 5 and 25 μM *p*-nitrophenol and 8 μM [^{35}S]3′-phosphoadenosine 5′-phosphosulfate by using the barium precipitation procedure (22).

Results

Inactivation of *Nas1*. Our targeting strategy (Fig. 1*A*) replaced *Nas1* exons 4–6 with a neomycin-resistance cassette. Genomic Southern analysis using both neomycin and external probes (Fig. 1 *B* and *C*) and PCR analysis (Fig. 1*D*) confirmed the targeted disruption of *Nas1* in ES cells. The genotypes of 435 mice were determined by PCR and Southern blot analysis (Fig. 1 *C* and *E*): 117 were *Nas1*$^{+/+}$ (27%), 209 *Nas1*$^{+/-}$ (48%), and 109 *Nas1*$^{-/-}$ (25%), which is close to the Mendelian ratio (1:2:1), indicating that loss of *Nas1* is not embryonically lethal. Northern hybridization revealed the presence of the two NaS_i-1 mRNA transcripts (2.5 and 2.2 kb) that are normally present in *Nas1*$^{+/+}$ kidney and ileum (13), and the two truncated (≈300 nucleotides smaller) transcripts (2.2 and 1.9 kb) in *Nas1*$^{-/-}$ mice (Fig. 2*D*). Sequence analysis of the truncated RT-PCR products from *Nas1*$^{-/-}$ mice (Fig. 2*B*) revealed sequence skipping from exon 3 to exon 7, with an in-frame stop codon at the junction of exons 3 and 7 (Fig. 2*A*). The truncated cDNA encodes the first 121 amino acids of the NaS_i-1 protein, which was unable to induce any Na^+–SO_4^{2-} cotransport in *Xenopus* oocytes (data not shown). Quantitation of the NaS_i-1 RT-PCR products, relative to β-actin, indicated that *Nas1*$^{+/-}$ mice had ≈50% of both wild-type and truncated NaS_i-1 mRNAs (Fig. 2*C*). The level of truncated NaS_i-1 mRNA in *Nas1*$^{-/-}$ mice, determined by densitometric analysis, was similar to the level of wild-type NaS_i-1 mRNA in *Nas1*$^{+/+}$ mice.

Characterization of the *Nas1* Knockout Mice. ***Membrane transport.*** To determine the effect of the *Nas1* null allele on functional activity, BBMVs were isolated from tissues where NaS_i-1 is highly expressed (renal cortex and ileal mucosa) from *Nas1*$^{+/+}$, *Nas1*$^{+/-}$, and *Nas1*$^{-/-}$ mice and flux transport measurements were performed. Na^+-dependent SO_4^{2-} uptake was abolished in ileal BBMVs and reduced (by 90%) in renal BBMVs from *Nas1*$^{-/-}$ mice, whereas an ≈50% reduction was observed in renal and ileal BBMVs from *Nas1*$^{+/-}$ mice, when compared with *Nas1*$^{+/+}$ mice (Fig. 3). Na^+-independent SO_4^{2-} uptake (Fig. 3) and Na^+-dependent glucose uptake (data not shown) was similar in *Nas1*$^{+/+}$, *Nas1*$^{+/-}$, and *Nas1*$^{-/-}$ mice. These data suggest that the reduced Na^+–SO_4^{2-} cotransport was due to the loss of a functional NaS_i-1 protein in the *Nas1*$^{-/-}$ mice. Our data also indicate that there is no compensation of the active *Nas1* allele in the *Nas1*$^{+/-}$ mice to compensate for the loss of one functional *Nas1* allele.

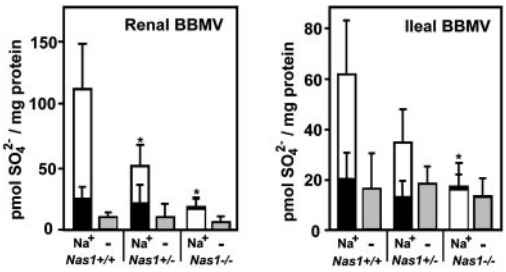

Fig. 3. Na^+–SO_4^{2-} uptake in renal and ileal BBMVs from *Nas1*$^{+/+}$, *Nas1*$^{+/-}$, and *Nas1*$^{-/-}$ mice. SO_4^{2-} uptake was measured in 100 mM NaCl for 10 s (white bars) and 90 min (black bars) or in 100 mM KCl for 10 s (*gray bars*). Each bar represents the mean ± SD of four measurements derived from each BBM preparation (12 *Nas1*$^{+/+}$, 12 *Nas1*$^{+/-}$, and 12 *Nas1*$^{-/-}$ mice) and is representative of two independent experiments. *, $P < 0.05$ when compared with *Nas1*$^{+/+}$.

Growth retardation. As an indicator of growth, we measured body weight and tail length of mice up to 24 weeks of age (Fig. 4). At birth, *Nas1*$^{-/-}$ males and females resembled *Nas1*$^{+/+}$ and *Nas1*$^{+/-}$ littermates in body weight. *Nas1*$^{-/-}$ mice were generally smaller than *Nas1*$^{+/+}$ and *Nas1*$^{+/-}$ mice at 1 week of age, although significant ($P < 0.05$) differences were not detected until week 2. From 19 litters, the average weights of *Nas1*$^{-/-}$ males and females at 3 weeks of age were 75 ± 3% ($P < 0.001$) and 76 ± 3% ($P < 0.001$), respectively, of the *Nas1*$^{+/+}$ and *Nas1*$^{+/-}$ littermates, and remained so for at least 5 months thereafter (Fig. 4). Tail lengths of *Nas1*$^{-/-}$ mice were shorter (by ≈10%) than *Nas1*$^{+/+}$ and *Nas1*$^{+/-}$ littermates (Fig. 4). In addition, at 4 weeks of age, the femoral length was decreased in *Nas1*$^{-/-}$ mice (0.91 ± 0.04 cm, $n = 8$; $P < 0.01$) when compared with *Nas1*$^{+/+}$ mice (1.03 ± 0.03 cm, $n = 8$). Taken together, these data demonstrated a growth retardation in *Nas1*$^{-/-}$ mice.

Reduced fertility. *Nas1*$^{-/-}$ male mice grew to become fertile animals, whereas female *Nas1*$^{-/-}$ mice showed a lower fertility than *Nas1*$^{+/+}$ and *Nas1*$^{+/-}$ littermates, with the average litter size for *Nas1*$^{-/-}$ females being 4.1 ± 3.9 ($n = 19, P < 0.001$), compared with *Nas1*$^{+/+}$ (10.7 ± 2.5, $n = 15$) and *Nas1*$^{+/-}$ (10.9 ± 1.8, $n = 18$) mice. In addition, blood spotting or miscarriages were observed in seven pregnancies from three of the *Nas1*$^{-/-}$ females at 14.6 ± 1.5 days postcoitum.

Seizures. We observed seizures in *Nas1*-deficient mice at ≈8 months of age. The stress of simply handling the mice could elicit a seizure in some of them. These episodes frequently included the mouse turning over onto a side position with clonic seizures, from which

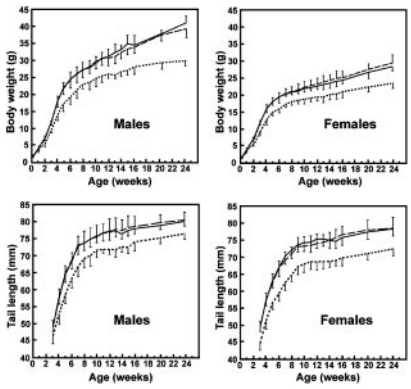

Fig. 4. Growth of *Nas1*$^{+/+}$, *Nas1*$^{+/-}$, and *Nas1*$^{-/-}$ mice. Body weights (*Upper*) and tail lengths (*Lower*) were determined for male and female mice up to 24 weeks of age. Each point represents the mean ± SD derived from 15–30 measurements of *Nas1*$^{+/+}$ (solid line), *Nas1*$^{+/-}$ (long dashed line), and *Nas1*$^{-/-}$ (dotted line) mice.

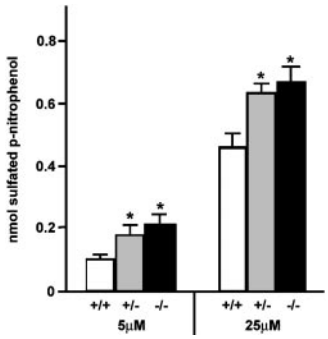

Fig. 5. Elevation of hepatic ST activity in *Nas1*-deficient mice. Phenol ST activities (mean ± SD, $n = 5$) in liver cytosol from $Nas1^{+/+}$ (white bars), $Nas1^{+/-}$ (gray bars), and $Nas1^{-/-}$ (black bars) mice. The concentrations of *p*-nitrophenol in the assays were 5 and 25 μM. *, $P < 0.01$ when compared with $Nas1^{+/+}$.

the mouse usually recovered within 2 min. The seizures were mostly observed in $Nas1^{-/-}$ mice (27%, $n = 26$), but were also observed in a small number of $Nas1^{+/-}$ mice (5%, $n = 43$).

Histology and organ phenotypes. Gross histological analysis of tissue sections of kidney, ileum, liver, heart, spleen, uterus, seminal vesicles, adrenals, bone, and skin from $Nas1^{-/-}$ and $Nas1^{+/+}$ mice at 4 and 48 weeks of age, respectively, showed no structural peculiarities (data not shown). However, we detected a small but significant increase in the liver:body weight ratio of $Nas1^{-/-}$ mice (5.31 ± 0.47%, $n = 14$; $P < 0.01$) when compared with $Nas1^{+/-}$ (4.67 ± 0.50%, $n = 18$) and $Nas1^{+/+}$ (4.57 ± 0.22%, $n = 9$) mice.

Liver cytosolic ST activity. ST activity was assayed in the *Nas1*-deficient mice to determine whether their low serum SO_4^{2-} levels were associated with changes in ST activity. The level of phenol ST activity was significantly ($P < 0.01$) increased in $Nas1^{-/-}$ (1.5- to 2.0-fold) and $Nas1^{+/-}$ (1.4- to 1.7-fold) mice when compared with their $Nas1^{+/+}$ littermates (Fig. 5). There was a small but nonsignificant increase in the average ST activity from the $Nas1^{-/-}$ mice (1.1-fold increase) when compared with the $Nas1^{+/-}$ mice (Fig. 5).

Blood and urinary data. Several blood and urine parameters of $Nas1^{-/-}$ mice were significantly different from their $Nas1^{+/+}$ littermates (Table 1). At all ages examined, the serum SO_4^{2-} concentration in $Nas1^{-/-}$ mice was markedly reduced by >75% ($P < 0.001$), whereas $Nas1^{+/-}$ mice exhibited an intermediate serum SO_4^{2-} concentration that was lower by >40% ($P < 0.001$) than that of $Nas1^{+/+}$ mice. Urine SO_4^{2-}:creatinine ratio and FEI for SO_4^{2-} were elevated in $Nas1^{-/-}$ mice when compared with $Nas1^{+/+}$ mice. The FEI for SO_4^{2-} was also increased in $Nas1^{+/-}$ mice. Serum creatinine levels were constant between genotypes (data not shown). Serum levels of PO_4^{2-}, Ca^{2+}, Na^+, K^+, and Cl^-, and urine levels of PO_4^{2-} and Ca^{2+} were similar in the $Nas1^{-/-}$, $Nas1^{+/-}$, and $Nas1^{+/+}$ mice (Table 1), showing that *Nas1* ablation specifically disrupted SO_4^{2-} homeostasis without affecting the homeostasis of other ions such as PO_4^{2-}, Ca^{2+}, Na^+, K^+, and Cl^-. Furthermore, there is no increase in urinary protein excretion in $Nas1^{-/-}$ mice (Table 1), indicating that a generalized tubulopathy was not responsible for the renal SO_4^{2-} leak in $Nas1^{-/-}$ mice. The values obtained for whole blood and urine pH were not different between the genotypes (Table 1). Consistent with the growth retardation of $Nas1^{-/-}$ mice, the serum level of IGFI was significantly reduced by >30% ($P < 0.001$) in the $Nas1^{-/-}$ mice when compared with the $Nas1^{+/+}$ mice (Table 1). Systolic blood pressure was not different ($P = 0.46$) between the $Nas1^{-/-}$ (132.4 ± 4.2 mmHg, $n = 7$) and $Nas1^{+/+}$ mice (132.9 ± 10.1 mmHg, $n = 7$).

Because bile acids require SO_4^{2-} conjugation for normal function (4), we measured serum bile acid levels in the $Nas1^{-/-}$, $Nas1^{+/-}$, and $Nas1^{+/+}$ littermates. Elevated levels of several different bile acids were found in the $Nas1^{-/-}$ and $Nas1^{+/-}$ mice (Table 2). Serum levels of cholic, hyodeoxycholic, murocholic, chenocholic, glycoursodeoxycholic, glycolithocholic, and taurocholic acid were significantly increased by ≈2- to 4-fold in the $Nas1^{-/-}$ mice, when compared with the $Nas1^{+/+}$ mice. The serum concentration of murocholic and taurocholic acids was increased by 2- and >4-fold,

PHYSIOLOGY

Table 1. Blood and urine profiles for $Nas1^{+/+}$, $Nas1^{+/-}$, and $Nas1^{-/-}$ mice

	Age, mo	$Nas1^{+/+}$ (*n*)	$Nas1^{+/-}$ (*n*)	$Nas1^{-/-}$ (*n*)
Serum SO_4^{2-}, mM	2	0.99 ± 0.23 (9)	0.56 ± 0.15 (8)**	0.22 ± 0.05 (11)**
	4	0.98 ± 0.10 (7)	0.57 ± 0.08 (8)**	0.22 ± 0.04 (12)**
Serum PO_4^{2-}, mM	2	2.39 ± 0.26 (9)	2.39 ± 0.30 (8)	2.37 ± 0.33 (11)
	4	1.97 ± 0.23 (7)	2.06 ± 0.18 (8)	2.08 ± 0.26 (12)
Serum total Ca^{2+}, mM	2	2.22 ± 0.14 (9)	2.22 ± 0.14 (8)	2.20 ± 0.16 (11)
	4	2.15 ± 0.06 (7)	2.18 ± 0.31 (8)	2.24 ± 0.26 (12)
Urine SO_4^{2-}/creatinine	2	8.91 ± 0.74 (9)	9.10 ± 0.88 (8)	10.01 ± 1.09 (11)*
	4	8.92 ± 0.75 (7)	9.06 ± 0.91 (8)	10.07 ± 1.03 (12)*
Urine PO_4^{2-}/creatinine	2	12.47 ± 4.18 (9)	12.47 ± 4.09 (8)	14.02 ± 4.81 (11)
	4	13.58 ± 4.07 (7)	11.54 ± 4.70 (8)	13.45 ± 5.00 (12)
Urine Ca^{2+}/creatinine	2	1.04 ± 0.30 (9)	0.96 ± 0.18 (8)	1.00 ± 0.30 (11)
	4	1.07 ± 0.32 (7)	0.96 ± 0.18 (8)	1.00 ± 0.29 (12)
FEI SO_4^{2-}	2	0.21 ± 0.05 (9)	0.38 ± 0.09 (8)**	1.09 ± 0.34 (11)**
	4	0.20 ± 0.03 (7)	0.37 ± 0.05 (8)**	1.07 ± 0.25 (12)**
FEI PO_4^{2-}	2	0.12 ± 0.05 (9)	0.12 ± 0.04 (8)	0.13 ± 0.05 (11)
	4	0.15 ± 0.05 (7)	0.13 ± 0.05 (8)	0.15 ± 0.05 (12)
FEI Ca^{2+}	2	0.010 ± 0.003 (9)	0.010 ± 0.002 (8)	0.010 ± 0.003 (11)
	4	0.011 ± 0.003 (7)	0.010 ± 0.002 (8)	0.011 ± 0.004 (12)
Urine total protein, ng/μl	2	2.62 ± 0.98 (9)	2.52 ± 0.81 (11)	2.01 ± 1.06 (6)
Urine pH	2	6.5 ± 0.6 (7)	7.1 ± 0.6 (7)	6.6 ± 0.6 (5)
Whole blood pH	2	7.4 ± 0.2 (7)	7.5 ± 0.1 (7)	7.3 ± 0.2 (5)
Serum IGF-I, ng/ml	2	421.9 ± 23.5 (4)	ND	280.6 ± 12.3 (4)**
	4	512.3 ± 37.9 (4)	ND	388.6 ± 15.1 (4)**
Serum Na^+, mM	2	144 ± 4 (7)	ND	143 ± 3 (7)
K^+, mM	2	6.9 ± 0.8 (7)	ND	6.3 ± 1.1 (6)
Cl^-, mM	2	111 ± 3 (7)	ND	110 ± 2 (6)

Results are means ± SD. ND, test not performed. *, $P < 0.05$ when compared with $Nas1^{+/+}$ mice. **, $P < 0.001$ when compared with $Nas1^{+/+}$ mice. FEI, ratio between {serum creatinine (mM) × urine SO_4^{2-}, PO_4^{2-}, or Ca^{2+} (mM)}/{urine creatinine (mM) × serum SO_4^{2-}, PO_4^{2-}, or Ca^{2+} (mM)}.

Table 2. Serum bile acid profiles for *Nas1*$^{+/+}$, *Nas1*$^{+/-}$, and *Nas1*$^{-/-}$ mice

Bile acid, nM	Age, mo	*Nas1*$^{+/+}$ (*n*)	*Nas1*$^{+/-}$ (*n*)	*Nas1*$^{-/-}$ (*n*)
Cholic	4	800 ± 540 (4)	3461 ± 2107 (4)	2987 ± 191 (4)*
Lithocholic	4	47.3 ± 14.2 (4)	70.9 ± 19.8 (4)	82.7 ± 29.6 (3)
Hyodeoxycholic	4	24.0 ± 2.5 (3)	40.5 ± 8.2 (3)	54.4 ± 9.4 (4)*
Ursodeoxycholic	4	345.7 ± 214.1 (4)	436.3 ± 4.7 (4)	296.2 ± 157.0 (4)
Murocholic	4	98.13 ± 28.0 (4)	204.5 ± 20.8 (4)**	290.1 ± 40.9 (4)**
Chenodeoxycholic	4	145.9 ± 64.2 (4)	241.4 ± 31.1 (4)	415.5 ± 72.1 (4)*
Deoxycholic	4	623 ± 326 (4)	1267 ± 637 (4)	904 ± 272 (4)
Glycoursodeoxycholic	4	2.6 ± 0.4 (3)	5.4 ± 1.9 (3)	6.6 ± 0.8 (4)*
Glycolithocholic	4	1.8 ± 0.7 (4)	1.3 ± 0.4 (3)	7.5 ± 3.5 (4)*
Taurocholic	4	5608 ± 4281 (4)	31442 ± 353 (4)*	24052 ± 3134 (4)*
Taurochenodeoxycholic	4	728 ± 339 (4)	785 ± 437 (4)	1157 ± 642 (4)
Taurodeoxycholic	4	287 ± 156 (4)	557 ± 429 (4)	740 ± 513 (4)

Results are means ± SD. *, $P < 0.05$ when compared with *Nas1*$^{+/+}$ mice. **, $P < 0.01$ when compared with *Nas1*$^{+/+}$ mice.

respectively, in *Nas1*$^{+/-}$ mice when compared with their *Nas1*$^{+/+}$ littermates.

Discussion

We have generated a *Nas1*-deficient mouse, which, to our knowledge, is the first model of an SO_4^{2-} transporter knockout. We demonstrated that the *Nas1*-deficient mice exhibited increased urinary SO_4^{2-} excretion and hyposulfatemia, together with increased serum bile acid levels. These features were associated with normal serum levels of PO_4^{2-}, Ca^{2+}, Na^+, K^+, and Cl^- and urine PO_4^{2-}:creatinine and Ca^{2+}:creatinine ratios and no changes in systolic blood pressure. In addition, the *Nas1*$^{-/-}$ mice have a growth retardation associated with decreased IGFI serum levels and display seizures in older mice.

The phenotypic features that characterize the *Nas1*$^{-/-}$ mice are likely the direct consequence of impaired SO_4^{2-} absorption and reabsorption, which is secondary to the loss of NaS_i-1 function in the intestine and kidney, respectively. This conclusion is based on our previous study (13), demonstrating that *Nas1* is strongly expressed in the ileum and kidney. Here, we demonstrate that Na^+–SO_4^{2-} cotransport is completely abolished in ileal BBMVs and reduced by 90% in renal BBMVs from *Nas1*$^{-/-}$ mice, suggesting that NaS_i-1 is the predominant Na^+–SO_4^{2-} cotransporter in kidney and intestine, and that other molecular entities that may contribute to SO_4^{2-} homeostasis, do not compensate for the lack of NaS_i-1. Because *Nas1*$^{-/-}$ mice have very low serum SO_4^{2-} levels (>75% reduction) and a 5-fold increase in FEI SO_4^{2-} when compared with wild-type littermates, the loss of the renal NaS_i-1 is most likely the primary cause of the hyposulfatemia in the *Nas1*$^{-/-}$ mice. However, the precise contribution of the intestinal NaS_i-1, relative to the renal NaS_i-1, to the serum SO_4^{2-} levels, will come from future studies that aim to measure the level of excreted sulfate in the stools of *Nas1*$^{-/-}$ mice and their *Nas1*$^{+/+}$ and *Nas1*$^{+/-}$ littermates. Although disruption of NaS_i-1 leads to a significant reduction in the circulating concentration of SO_4^{2-}, it is interesting to note that this level is not completely abolished in the *Nas1*$^{-/-}$ mice. The remaining SO_4^{2-} level could possibly be obtained directly from the diet by other SO_4^{2-} transporters, including DRA (15) or DTDST (23). This finding is consistent with our BBMV data that shows a residual level of SO_4^{2-} transport, which may be due to DRA (1) or other transporters, which have yet to be identified. Alternatively, the remaining SO_4^{2-} could be derived from the sulfur-containing amino acids, cysteine and methionine (3). Nonetheless, our data demonstrate that *Nas1* plays a major role in the maintenance of serum SO_4^{2-} levels.

The *Nas1*$^{-/-}$ mice appear normal at birth, and the frequency of *Nas1* genotypes among the progeny from *Nas1*$^{+/-}$ × *Nas1*$^{+/-}$ matings is consistent with Mendelian inheritance. This finding shows that *Nas1* is not required for embryonic development, which is consistent with a gene array study of the developing rat kidney that showed an initial induction of NaS_i-1 mRNA levels at birth with increasing levels in the postnatal period (24). It is also consistent with intestine and kidney development, which occur late in gestation. An analysis of postnatal growth revealed a decrease of ≈25% in mean body weight and ≈10% in tail length of both male and female *Nas1*$^{-/-}$ mice. Growth retardation appears within the first few weeks after birth and is not compensated in adulthood. Consistent with the growth retardation in *Nas1*$^{-/-}$ mice is the 30% reduction in their serum IGFI levels. Lupu *et al.* (25) demonstrated the important role of IGFI in postnatal growth, mainly between 15 and 40 days of mouse age, which is consistent with the reduced IGFI levels and growth retardation of *Nas1*$^{-/-}$ mice between 2–6 weeks of age. Also consistent with the reduced IGFI level in the *Nas1*$^{-/-}$ mice is an ≈10% decrease in their femoral length when compared with *Nas1*$^{+/+}$ mice. Reductions in serum IGFI and femoral length were also observed in the liver IGFI-deficient (LID) mouse, acid labile subunit knock-out (ALSKO) mouse, and in the double gene disrupted LID plus ALSKO mouse (26). IGFI was reported to play a role in up-regulating the steady-state levels of NaS_i-1 mRNA and Na^+-SO_4^{2-} cotransport in cultured renal cells (27), and stimulating cartilage SO_4^{2-} uptake in *Xenopus* tadpoles (28). However, to our knowledge, the present study is the first to report that hyposulfatemia is associated with reduced levels of circulating IGFI.

We found significant increases in the levels of serum cholic, hyodeoxycholic, murocholic, chenocholic, glycoursodeoxycholic, glycolithocholic, and taurocholic acids in *Nas1*$^{-/-}$ mice, which indicates a disturbance in bile acid homeostasis. Bile acids play an important role in the intestinal absorption of lipids and lipid-soluble nutrients, with SO_4^{2-} conjugation being an important modification for maintaining normal levels of bile acids in the intestine (4). SO_4^{2-} conjugation was also shown to protect ursodeoxycholic acid from bacterial degradation in the intestine (29), which may explain why this particular bile acid was not elevated in the serum from *Nas1*$^{-/-}$ mice. Consistent with the 16% increase in liver:body weight ratio in the *Nas1*$^{-/-}$ mice, when compared with *Nas1*$^{+/+}$ mice, Repa *et al.* (30) described hepatomegaly and disturbed bile acid homeostasis in *cyp27*$^{-/-}$ mice. We speculate that the low availability of SO_4^{2-} in *Nas1*$^{-/-}$ mice may disturb normal bile acid homeostasis and lead to hepatomegaly.

Nas1$^{-/-}$ female mice showed a reduced fertility, which was not seen in the male *Nas1*$^{-/-}$ mice. Our data shows that litter sizes of female *Nas1*$^{-/-}$ mice at birth were ≈60% lower than litters from either *Nas1*$^{+/+}$ or *Nas1*$^{+/-}$ mice. Early studies (31, 32) showed that serum SO_4^{2-} levels increased during pregnancy, which were correlated with an increased renal reabsorption of SO_4^{2-} (33). More recently, BBMV Na^+–SO_4^{2-} cotransport was observed to be higher in pregnant guinea pigs when compared with nonpregnant animals (34). We observed blood spotting and miscarriages in some *Nas1*$^{-/-}$ mice at ≈14 days gestation, which corresponds to the beginning of

the third trimester. These observations could be ascribed to the low sulfatemia in the *Nas1*$^{-/-}$ mice. A number of changes of sulfated compounds take place in the endometrium during pregnancy, including increased turnover of heparan sulfate proteoglycans (35), delocalization of syndecan (36), and a change in the cholesterol sulfate levels (37). In addition, Mi *et al.* (38) demonstrated the importance of the sulfated lutropin (LH) receptor, mannose/*N*-acetylgalactosamine-4-SO_4, in maintaining normal serum levels of LH during pregnancy. More recently, tyrosylprotein ST-1-deficient mice were shown to have smaller litter sizes as a result of increased postimplantation fetal death (39). These observations, together with the findings of the present study, indicate that SO_4^{2-} is important for female reproductive physiology.

The seizure susceptibility phenotype of the *Nas1*-deficient mice underscores the important, yet poorly understood role of SO_4^{2-} in mammalian neurology. Seizures are a common feature in some human syndromes of disturbed SO_4^{2-} metabolism. These include metachromatic leukodystrophy (40) and Hunter's syndrome (41), which are caused by a deficiency in cerebroside sulfatase and iduronate-2-sulfatase activity, respectively. In addition, catecholamines display anticonvulsant properties (reviewed in ref. 42), and SO_4^{2-} conjugation is required for maintaining their circulating levels. Strobel *et al.* (43) showed that catecholamine sulfates exhibit a plasma half-life of ≈3 h, which is in contrast to free catecholamines with a half-life of <3 min. The mode of inheritance of seizures in mammals is variable, with evidence for both Mendelian and more complex patterns of inheritance (44). Our observation of seizures in a small number (≈5%) of *Nas1*$^{+/-}$ mice indicates a complex pattern of inheritance, which may be influenced by the mixed genetic background of the mice in this present study. The intriguing finding of seizures in hyposulfatemic mice represents an important area for future research.

The phenotype of the *Nas1*$^{+/-}$ mice is of great interest. *Nas1*$^{+/-}$ mice grow normally, despite the ≈50% reduction in their Na^+–SO_4^{2-} cotransport activity, leading to a 50% reduction in their serum SO_4^{2-} levels. These findings indicate that the normal *Nas1* allele in *Nas1*$^{+/-}$ mice does not compensate for the loss of one functional *Nas1* allele. Although *Nas1* is weakly expressed in other tissues including testis, adrenal, and adipose tissue (13), these tissues do not appear to contribute to the circulating levels of SO_4^{2-}. The subtle phenotype of the *Nas1*$^{+/-}$ mice, in comparison to the *Nas1*$^{-/-}$ mice, implies that the level of sulfatemia should reach a threshold between 0.22 and 0.56 mM before it has an affect on growth and fertility.

Interestingly, our data show an increase of liver phenol ST activity in both *Nas1*$^{-/-}$ and *Nas1*$^{+/-}$ mice. Although glucocorticoids and some clinical conditions such as diabetes have been shown to increase ST gene expression (45), no studies to date have examined the effect of reduced SO_4^{2-} levels in the body on ST activity. Our data indicate that ST activity is sensitive to changes in blood SO_4^{2-} levels and is positively regulated, even with intermediate reductions of serum SO_4^{2-} levels, as shown in the *Nas1*$^{+/-}$ mice.

In summary, the generation and characterization of a *Nas1*$^{-/-}$ mouse has underscored the essential role of the NaS_i-1 transporter in maintaining SO_4^{2-} homeostasis, normal development and growth, and highlights the importance of SO_4^{2-} in mammalian biology. The *Nas1* knockout mouse now provides an animal model for defining the effects of disturbed sulfate homeostasis on a variety of organ systems where sulfate plays an important physiological role.

We thank Dr. I. Wilkie (School of Veterinary Science, University of Queensland) for the histopathological analyses, Dr. P. Noakes and N. Hemple (School of Biomedical Sciences, University of Queensland) for valuable discussions, and Associate Professor C. Liddle and S. Coulter (Department of Clinical Pharmacology and Storr Liver Unit, Westmead Millennium Institute, University of Sydney, Sydney) for performing the bile acid measurements. This work was supported in part by the Australian Research Council and the National Health and Medical Research Council (D.M., L.B., and P.A.D.).

1. Markovich, D. (2001) *Physiol. Rev.* **81,** 1499–1534.
2. Falany, C. N. (1997) *FASEB J.* **11,** 206–216.
3. Mulder, G. J. (1981) in *Sulfation of Drugs and Related Compounds*, ed. Mulder, G. J. (CRC, Boca Raton, FL), pp. 32–52.
4. Mulder, G. J. & Jakoby, W. B. (1990) in *Conjugation Reactions in Drug Metabolism: An Integrated Approach*: *Substrates*, *Cosubstrates*, *Enzymes*, *and Their Interactions In Vivo and In Vitro*, ed. Mulder, G. J. (Taylor and Francis, London), pp. 107–161.
5. Hastbacka, J., Superti-Furga, A., Wilcox, W. R., Rimoin, D. L., Cohn, D. H. & Lander, E. S. (1996) *Am. J. Hum. Genet.* **58,** 255–262.
6. Tallgren, L. (1980) *Acta Med. Scand. Suppl.* **640,** 1–100.
7. Murer, H., Manganel, M. & Roch-Ramel, F. (1992) in *Handbook of Physiology*, ed. Winhager, E. (Oxford Univ. Press, London), Vol. 2, pp. 2165–2188.
8. Markovich, D., Forgo, J., Stange, G., Biber, J. & Murer, H. (1993) *Proc. Natl. Acad. Sci. USA* **90,** 8073–8077.
9. Becker, E. L., Heinemann, H. O., Igarashi, K., Holdler, J. E. & Gershberg, H. (1960) *J. Clin. Invest.* **39,** 1909–1913.
10. Berglund, F. & Sorbo, B. (1960) *Scand. J. Clin. Lab. Invest.* **12,** 147–153.
11. Krijgsheld, K. R., Scholtens, E. & Mulder, G. J. (1980) *Comp. Biochem. Physiol.* **67,** 683–686.
12. Dawson, P. A. & Markovich, D. (2002) *Cell Biochem. Biophys.* **36,** 175–182.
13. Beck, L. & Markovich, D. (2000) *J. Biol. Chem.* **275,** 11880–11890.
14. Lee, A., Beck, L. & Markovich, D. (2000) *Genomics* **70,** 354–363.
15. Hoglund, P., Haila, S., Socha, J., Tomaszewski, L., Saarialho-Kere, U., Karjalainen-Lindsberg, M., Airola, K., Holmberg, C., de la Chappelle, A. & Kere, J. (1996) *Nat. Genet.* **14,** 316–319.
16. Girard, J. P., Baekkevold, E. S., Feliu, J., Brandtzaeg, P. & Amalric, F. (1999) *Proc. Natl. Acad. Sci. USA* **96,** 12772–12777.
17. Tybulewicz, V., Crawford, C., Jackson, P., Bronson, R. & Mulligan, R. (1991) *Cell* **65,** 1153–1163.
18. Watson, A. J., Hogan, A., Hahnel, A., Wiemer, K. E. & Schultz, G. A. (1992) *Mol. Reprod. Dev.* **31,** 87–95.
19. Tenenhouse, H. S. & Scriver, C. R. (1978) *Can. J. Biochem.* **56,** 640–646.
20. Falany, J. L., Greer, H., Kovavs, T., Sorscher, E. J. & Falany, C. N. (2002) *Biochem. J.* **364,** 115–120.
21. Bradford, M. M. (1976) *Anal. Biochem.* **72,** 248–325.
22. Falany, C. N., Vazquez, M. E., Heroux, J. A. & Roth, J. A. (1990) *Arch. Biochem. Biophys.* **278,** 312–318.
23. Hastbacka, J., de la Chapelle, A., Mahtani, M., Clines, G., Reeve-Daly, M., Daly, M., Hamilton, B., Kusumu, K., Trivedi, B., Weaver, A., *et al.* (1994) *Cell* **78,** 1073–1087.
24. Stuart, R. O., Bush, K. T. & Nigam, S. K. (2001) *Proc. Natl. Acad. Sci. USA* **98,** 5649–5654.
25. Lupu, F., Terwilliger, J. D., Lee, K., Segre, G. V. & Efstratiadis, A. (2001) *Dev. Biol.* **229,** 141–162.
26. Yakar, S., Rosen, C. J., Beamer, W. G., Ackert-Bicknell, C. L., Wu, Y., Liu, J. L., Ooi, G. T., Setser, J., Frystyk, J., Boisclair, Y. R. & LeRoith, D. (2002) *J. Clin. Invest.* **110,** 771–781.
27. Lee, H. J., Sagawa, K., Shi, W., Murer, H. & Morris, M. E. (2000) *Proc. Soc. Exp. Biol. Med.* **225,** 49–57.
28. Schneider, A. & Hanke, W. (1997) *Comp. Biochem. Physiol. C Pharmacol. Toxicol. Endocrinol.* **117,** 317–322.
29. Rodrigues, C. M., Kren, B. T., Steer, C. J. & Setchell, K. D. (1995) *Gastroenterology* **109,** 2036–2038.
30. Repa, J. J., Lund, E. G., Horton, J. D., Leitersdorf, E., Russell, D. W., Dietschy, J. M. & Turley, S. D. (2000) *J. Biol. Chem.* **275,** 39685–39692.
31. Morris, M. E. & Levy, G. (1983) *J. Pharm. Sci.* **72,** 715–716.
32. Cole, D. E., Baldwin, L. S. & Stirk, L. J. (1985) *Clin. Chem.* **31,** 866–867.
33. Cole, D. E., Baldwin, L. S. & Stirk, L. J. (1985) *Obstet. Gynecol.* **66,** 485–490.
34. Lee, H. J., Balasubramanian, S. V. & Morris, M. E. (1999) *Proc. Soc. Exp. Biol. Med.* **221,** 336–344.
35. Morris, J. E., Potter, S. W. & Gaza-Bulseco, G. (1988) *J. Biol. Chem.* **263,** 4712–4718.
36. Potter, S. W. & Morris, J. E. (1992) *Anat. Rec.* **234,** 383–390.
37. Momoeda, M., Taketani, Y., Mizuno, M., Iwamori, M. & Nagai, Y. (1991) *Biochem. Biophys. Res. Commun.* **178,** 145–150.
38. Mi, Y., Shapiro, S. D. & Baenziger, J. U. (2002) *J. Clin. Invest.* **109,** 269–276.
39. Ouyang, Y. B., Crawley, J. T., Aston, C. E. & Moore, K. L. (2002) *J. Biol. Chem.* **277,** 23781–23787.
40. Bostantjopoulou, S., Katsarou, Z., Michelakaki, H. & Kazis, A. (2000) *Acta Neurol. Scand.* **102,** 192–195.
41. Wraith, J. E., Cooper, A., Thornley, M., Wilson, P. J., Nelson, P. V., Morris, C. P. & Hopwood, J. J. (1991) *Hum. Genet.* **87,** 205–206.
42. Weinshenker, D. & Szot, P. (2002) *Pharmacol. Ther.* **94,** 213–233.
43. Strobel, G., Friedmann, B., Jost, J. & Bartsch, P. (1994) *Am. J. Physiol.* **267,** E537–E543.
44. Kaneko, S., Okada, M., Iwasa, H., Yamakawa, K. & Hirose, S. (2002) *Neurosci. Res.* **44,** 11–30.
45. Runge-Morris, M. A. (1997) *FASEB J.* **11,** 109–117.